Numer. Math. (1999) 84: 143–171
Digital Object Identifier (DOI) 10.1007/s002119900098

Numerische Mathematik


# A residual based error estimator for mortar finite element discretizations

**Barbara I. Wohlmuth**

Universität Augsburg, Institut für Mathematik, Universitätsstrasse 14,
D-86159 Augsburg, Germany; (e-mail: wohlmuth@math.uni-augsburg.de)

Received July 18, 1997 / Revised version received July 27, 1998 /
Published online September 7, 1999

**Summary.** A residual based error estimator for the approximation of linear elliptic boundary value problems by nonconforming finite element methods is introduced and analyzed. In particular, we consider mortar finite element techniques restricting ourselves to geometrically conforming domain decomposition methods using P1 approximations in each subdomain. Additionally, a residual based error estimator for Crouzeix-Raviart elements of lowest order is presented and compared with the error estimator obtained in the more general mortar situation. It is shown that the computational effort of the error estimator can be considerably reduced if the special structure of the Lagrange multiplier is taken into account.

*Mathematics Subject Classification (1991):* 65N15, 65N30, 65N50, 65N55

## 1. Introduction

We will consider the following model problem

$$Lu := -\mathrm{div}\,(a\nabla u) + b\,u = f \quad \text{in } \Omega, \qquad u = 0 \quad \text{on } \Gamma := \partial\Omega \tag{1.1}$$

where $\Omega$ is a bounded, polygonal domain in $\mathbb{R}^2$ and $f \in L^2(\Omega)$. Furthermore, we assume $a = (a_{ij})_{i,j=1}^2$ to be a symmetric, uniformly positive definite matrix-valued function with $a_{ij} \in L^\infty(\Omega)$, $1 \le i,j \le 2$, and $0 \le b \in L^\infty(\Omega)$. The largest eigenvalue of $a$ restricted to a subset $D \subset \Omega$ is denoted by $\alpha_D$.

The paper is organized as follows: In Sect. 2, we consider the mortar finite element method for the special case of coupling conforming P1 finite element methods on nonmatching simplicial triangulations. Generally, each subdomain can be associated with different discretization techniques and or different triangulations. The mortar finite element method is a domain decomposition technique which requires no pointwise continuity across the interface between the subdomains; a characteristic feature of this method is that the solutions on the subdomains are only coupled in a weak sense.
A residual based error estimator is studied in Sect. 3. The main technical problem results from the discontinuity of the mortar finite element solution across the boundaries of the subdomains. To obtain satisfactory upper and lower bounds for the discretization error, we have to take the nonconformity of the mortar finite element solution into account.
In Sect. 4, we consider the Crouzeix-Raviart finite elements of lowest order associated with a simplicial regular triangulation on the whole domain $\Omega$. We analyze a residual based error estimator and observe that it has exactly the same structure as the error estimator studied in Sect. 3. The characteristic feature of both error estimators is a weighted $L^2$-norm of the jump of the finite element solution across the subdomain boundaries. We show that this part provides an appropriate measure of the nonconformity of the finite element solution.
In Sect. 5, we interpret the Crouzeix-Raviart discretization as a mortar finite element method. We show the local equivalence of the error estimators introduced in Sects. 3 and 4 and analyze the relation between the Lagrange multiplier and the normal derivative of the Crouzeix-Raviart finite element solution. The main result of this section provides a simplified error estimator which is locally equivalent to the original ones.
Finally, in Sect. 6 we present some numerical results illustrating the adaptive refinement process as well as the efficiency of the error estimators. We consider cases with boundary layers and with discontinuous coefficients. In the first case, we obtain an almost matching triangulation. However, there is a sharp interface between adaptive refined and unrefined regions in the second case because of the discontinuity of the coefficients.

## 2. A mortar finite element discretization

A description of a mortar finite element method begins with a decomposition of the initial domain $\Omega$ into non-overlapping subdomains $\Omega_k$, $1 \leq k \leq K$,

$$\overline{\Omega} = \bigcup_{k=1}^{K} \overline{\Omega}_k \quad \text{with } \Omega_l \cap \Omega_k = \emptyset, \;\; k \neq l.$$

Without loss of generality, we assume that the subdomains are polygons. We restrict ourselves to the geometrical conforming situation where the intersection between the boundary of two different subdomains $\partial\Omega_l \cap \partial\Omega_k$, $k \neq l$ as well as $\partial\Omega_l \cap \partial\Omega$ is either empty, a vertex, or a common edge (see Fig. 2.1).

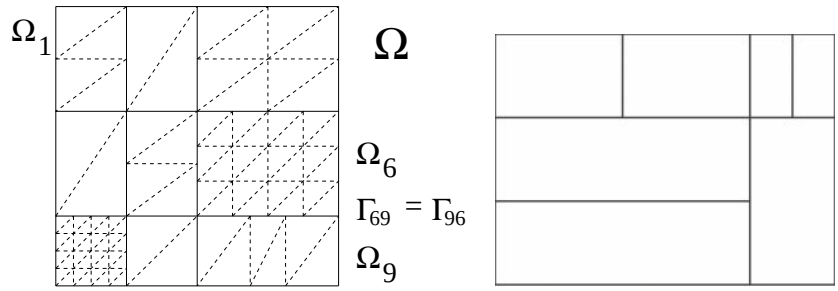


**Fig. 2.1.** Geometrically conforming (left) and nonconforming (right) situation

If two subdomains $\Omega_l$ and $\Omega_k$ have a common side, the intersection is called an interface and is denoted by $\overline{\Gamma}_{lk} = \overline{\Gamma}_{kl} := \partial\Omega_l \cap \partial\Omega_k$. $\boldsymbol{n}_{lk}$ stands for the unit normal vector from $\Omega_l$ to $\Omega_k$. The union of all interfaces is called the skeleton $\mathcal{S} := \bigcup_{k,l=1}^{K} \overline{\Gamma}_{lk}$.

An arbitrary discretization scheme can be used on each subdomain for the numerical solution of (1.1). Across the interface $\Gamma_{lk}$, the discrete solutions have to satisfy adequate matching conditions. A number of cases have been analyzed such as the coupling of different finite element methods, the coupling of spectral and finite element methods, and the combination of boundary element methods with finite element methods; see [1,4,5,14–17, 23,27,28,32].

A lot of work has also been done recently on the construction of efficient iterative solvers based on multilevel techniques [1–3,23,31,33,34]. In contrast, there are so far only a few papers considering adaptive refinement techniques and a posteriori error estimators [18,36].

A regular simplicial triangulation $\mathcal{T}_{h_k}$ is associated to each subdomain $\Omega_k$, $1 \leq k \leq K$. Let $\mathcal{E}_{h_k}$ and $\mathcal{P}_{h_k}$ denote the sets of edges and vertices of the triangulation $\mathcal{T}_{h_k}$, respectively. The sets of all triangles, vertices and edges are denoted by $\mathcal{T}_h$, $\mathcal{P}_h$, and $\mathcal{E}_h$, respectively.

In the following, we refer to $S_1(\Omega_k; \mathcal{T}_{h_k})$ as the standard conforming P1 finite element space defined locally on $\Omega_k$ by

$$S_1(\Omega_k; \mathcal{T}_{h_k}) := \{v \in C(\Omega_k) \mid \ v|_T \in P_1(T),\ T \in \mathcal{T}_{h_k},\ v|_{\partial\Omega \cap \partial\Omega_k} = 0\}\,.$$

Then, the global discrete space $X_h^{-1}(\Omega)$ is defined by

$$X_h^{-1}(\Omega) := \prod_{k=1}^{K} S_1(\Omega_k; \mathcal{T}_{h_k}).$$

In general, a function $v \in X_h^{-1}(\Omega)$ will be discontinuous across the skeleton $\mathcal{S}$.

Typically, a priori error estimates of a finite element solution involve two terms: the approximation error and the consistency error. If we use the global space $X_h^{-1}(\Omega)$ as the finite element ansatz space, the approximation error would be of order $O(h)$, but since $X_h^{-1}(\Omega)$ requires no continuity across the interfaces, the consistency error would be unlimited.

To define an appropriate finite element ansatz space, we have to introduce some matching conditions across the skeleton of the decomposition. In particular, a weak continuity condition has to be imposed on each interface. This can be done by using Lagrange multipliers on the skeleton. Before proceeding further, we have to consider the skeleton $\mathcal{S}$ in more detail. For each interface of the skeleton $\Gamma_{ij} = \Gamma_{ji}$, we choose one of the two associated subdomains, either $\Omega_i$ or $\Omega_j$. Here, we will select without loss of generality $\Omega_j$. The finite dimensional space given by the trace of functions in $S_1(\Omega_j; \mathcal{T}_{h_j})$ restricted on $\Gamma_{ij}$ is then called the mortar space and the opposite side is called non-mortar side. Now, the skeleton can be directly decomposed in

$$\begin{aligned}
\mathcal{S} &= \bigcup_{e \in \mathcal{E}_{\mathrm{L}}} e, \\
\mathcal{E}_{\mathrm{L}} &:= \{e \in \mathcal{E}_h |\ \exists i, j\ \ 1 \le i \le K,\ j \in \mathcal{M}(i)\ \text{ such that }\ e \in \mathcal{E}_{h_i} \cap \Gamma_{ij}\} \\
\mathcal{S} &= \bigcup_{e \in \mathcal{E}_{\mathrm{M}}} e, \\
\mathcal{E}_{\mathrm{M}} &:= \{e \in \mathcal{E}_h |\ \exists i, j\ \ 1 \le i \le K,\ j \in \mathcal{M}(i)\ \text{ such that }\ e \in \mathcal{E}_{h_j} \cap \Gamma_{ij}\}
\end{aligned}$$

where $\mathcal{M}(i) := \{1 \le j \le K |$ the mortar space on $\Gamma_{ij}$ inheriting its 1D mesh from $\mathcal{T}_{h_j}$ on $\Omega_j\}$. The set $\mathcal{M}(i)$ can be empty. We introduce appropriate matching conditions on the skeleton by means of the space $W_h(\mathcal{S}) \subset L^2(\mathcal{S})$ of Lagrange multipliers

$$\begin{aligned}
W_h(\mathcal{S}) &:= \prod_{i=1}^{K} \prod_{j \in \mathcal{M}(i)} W(\Gamma_{ij}; \mathcal{T}_{h_i}), \\
W(\Gamma_{ij}; \mathcal{T}_{h_i}) &:= \big\{\mu \in L^2(\Gamma_{ij}) \,|\ \ \mu = w|_{\Gamma_{ij}},\ \ w \in S_1(\Omega_i; \mathcal{T}_{h_i}), \\
&\qquad w|_e = \text{const.}, \text{ if } e \text{ contains an endpoint of } \Gamma_{ij},\ e \in \mathcal{E}_{\mathrm{L}}\big\}.
\end{aligned}$$

Note that the Lagrange multiplier space on $\Gamma_{ij}$, $j \in \mathcal{M}(i)$ is associated with the non-mortar side in contrast to the mortar space. The space for the mortar finite element method is now defined as

$$X_h(\Omega) := \left\{v \in X_h^{-1}(\Omega) \,|\ \ b\,(\mu, v) = 0,\ \ \mu \in W_h(\mathcal{S})\right\},$$

where the bilinear form $b(\cdot,\cdot)$ is given by

$$b(\mu,w) := -\sum_{i=1}^{K}\sum_{j\in\mathcal{M}(i)}\int_{\Gamma_{ij}}\mu\,[w]_J\,d\sigma,\quad w\in\prod_{i=1}^{K}H^1(\Omega_i),\ \mu\in L^2(\mathcal{S}),$$

and the jump on $\Gamma_{ij}$, $j\in\mathcal{M}(i)$ by $[w]_J := w|_{\Omega_i} - w|_{\Omega_j}$.

The mortar finite element solution $u_{\mathrm{M}}\in X_h(\Omega)$ is defined as the unique solution of the following discrete variational problem

$$a(u_{\mathrm{M}},v) = (f,v)_0,\quad v\in X_h(\Omega), \tag{2.1}$$

where $a(\cdot,\cdot)$,

$$\begin{aligned} a(v,w) &:= \sum_{i=1}^{K} a_i(v,w),\\ a_i(v,w) &:= \int_{\Omega_i} a\nabla v\cdot\nabla w + b\,vw\,dx,\quad v,w\in\prod_{i=1}^{K}H^1(\Omega_i), \end{aligned}$$

defines the discrete bilinear form, and the broken energy norm is given by $|||v|||^2 := a(v,v)$. If we use the primal hybrid formulation, the variational problem yields the following saddle point problem: Find $(u_{\mathrm{M}},\lambda_{\mathrm{M}})\in X_h^{-1}(\Omega)\times W_h(\mathcal{S})$ such that

$$\begin{aligned} a(u_{\mathrm{M}},v) + b(\lambda_{\mathrm{M}},v) &= (f,v)_0, && v\in X_h^{-1}(\Omega)\\ b(\mu,u_{\mathrm{M}}) &= 0, && \mu\in W_h(\mathcal{S}) \end{aligned} \tag{2.2}$$

is satisfied. Because of the second equation of the saddle point problem, the solution of (2.1) and the first component of the solution of (2.2) are the same. If the solution $u$ is smooth enough, the following a priori estimate is well known

$$|||u-u_{\mathrm{M}}|||^2 \le C\sum_{i=1}^{K} h_i^2\|u\|^2_{2;\Omega_i};$$

(see [16–18] and the references therein). In the following, we will use the constants $0<c$, $C<\infty$ as generic constants which only depend on the initial coarse triangulation, the local ratio of the smallest and largest eigenvalues of $a$ and the local ratio of $bh^2$ and the largest eigenvalue of $a$, but not on the refinement level or the element $T\in\mathcal{T}_h$.

## 3. A residual based error estimator

In this section, we introduce an error estimator which is based on the dual norm of the residual. We recall that the concept of residual based error estimation can be found in the early work of Babuška and Rheinboldt [8,9] and has been further developed by others [12,13,26,39]. These estimators are well established for conforming, nonconforming Crouzeix-Raviart, and mixed finite elements. An overview of the concepts and techniques for the conforming setting is given in [19,40], whereas [6,20–22,25,29,30,38,41] refer to more general variational formulations.

If the weak solution of (1.1) $u$ is contained in $\prod_{i=1}^{K} H^2(\Omega_i)$ and the jump of the normal derivative $a\nabla u \cdot \boldsymbol{n}$ vanishes on the skeleton, then it can be easily seen, by using Green's formula, that the error satisfies a continuous variational problem

$$a\,(u - u_{\mathrm{M}}, v) = r(v), \quad v \in \prod_{i=1}^{K} H^1(\Omega_i) \tag{3.1}$$

where the residual $r$ is given by $r(v) := (f, v)_0 - b\,(\lambda, v) - a\,(u_{\mathrm{M}}, v)$ with $\lambda|_{\Gamma_{ij}} := a\nabla u \cdot \boldsymbol{n}_{ij}$, $1 \le i \le K$, $j \in \mathcal{M}(i)$.

### *3.1. A saturation assumption*

A weighted norm $\|\cdot\|_{\mathrm{L}}$ on the skeleton is given by $\|v\|_{\mathrm{L}}^2 := \sum_{e \in \mathcal{E}_{\mathrm{L}}} h_e \alpha_e^{-1} \cdot \|v\|_{0;e}^2$. Here $\alpha_e := \alpha_T$, if $e$ is an edge of $T \in \mathcal{T}_{h_i}$ and $\alpha_e := 0.5(\alpha_{T_1} + \alpha_{T_2})$ if $e$ is an interior edge $e \in \mathcal{E}_h \setminus \mathcal{S}$, $e = \partial T_1 \cap \partial T_2$. If the solution $(u, \lambda)$ is smooth enough, the energy norm of the error $|||u - u_{\mathrm{M}}|||$ is of order $O(h)$ (see e.g. [16–18]) whereas $\inf_{\mu \in W_h(\mathcal{S})} \|\lambda - \mu\|_{\mathrm{L}}$ is at least of order $O(h^{3/2})$. To some extent, these a priori estimates justify the following saturation assumption

$$\inf_{\mu \in W_h(\mathcal{S})} \|\lambda - \mu\|_{\mathrm{L}} \le C_h |||u - u_{\mathrm{M}}|||, \quad C_h > 0 \tag{3.2}$$

with $C_h \le C_0 < \infty$ for $h \to 0$.

**Lemma 3.1** *Under the saturation assumption (3.2), there exists a constant* $C_{\lambda_{\mathrm{M}}} > 0$ *independent of the refinement level such that*

$$\|\lambda - \lambda_{\mathrm{M}}\|_{\mathrm{L}} \le C_{\lambda_{\mathrm{M}}} |||u - u_{\mathrm{M}}|||.$$

*Proof.* We obtain, from the triangle inequality,

$$\|\lambda - \lambda_{\mathrm{M}}\|_{\mathrm{L}} \le \inf_{\mu \in W_h(\mathcal{S})} \left(\|\lambda - \mu\|_{\mathrm{L}} + \|\mu - \lambda_{\mathrm{M}}\|_{\mathrm{L}}\right).$$

In view of the saturation assumption (3.2), we need only consider the second term of the right hand side further. By construction of the discrete space of Lagrange multipliers, $\lambda_{\mathrm{M}}$ is not necessarily continuous at the crosspoints of the skeleton. It is therefore in general not possible to find a $v \in X_h^{-1}(\Omega)$ such that $[v]_J = \lambda_{\mathrm{M}}$ on the skeleton or such that $\|\lambda_{\mathrm{M}}\|_{\mathrm{L}} \cdot \|[v]_J\|_{\mathrm{L}^{-1}} = b(\mu, v)$, where $\|v\|^2_{\mathrm{L}^{-1}} := \sum_{e\in\mathcal{E}_{\mathrm{L}}} \frac{\alpha_e}{h_e}\|v\|^2_{0;e}$. By using $\lambda_{\mathrm{M}}|_e = \mathrm{const.}$ on the edges $e$ containing one endpoint of the interfaces, the weighting factors, the inverse inequality for polynomials and (2.2), we obtain

$$
\begin{aligned}
&\|\mu - \lambda_{\mathrm{M}}\|_{\mathrm{L}} \\
&\le C \sup_{v\in\tilde{X}_h^{-1}(\Omega)} b(\mu - \lambda_{\mathrm{M}}, v) \cdot \| [v]_J \|^{-1}_{\mathrm{L}^{-1}} \\
&\le C\Big( \sup_{v\in\tilde{X}_h^{-1}(\Omega)} \inf_{\substack{w\in X_h^{-1}(\Omega)\\ [w]_J=[v]_J}} a(u_{\mathrm{M}} - u, w) \cdot \| [w]_J \|^{-1}_{\mathrm{L}^{-1}} + \|\lambda - \mu\|_{\mathrm{L}}\Big) \\
&\le C\left( |\!|\!| u_{\mathrm{M}} - u |\!|\!| + \|\lambda - \mu\|_{\mathrm{L}}\right),
\end{aligned}
$$

where $\tilde{X}_h^{-1}(\Omega) := \{v \in X_h^{-1}(\Omega) \,|\, (v|_{\Omega_j})|_{\Gamma_{ij}} = 0,\ 1 \le i \le k,\ j \in \mathcal{M}(i)\}$. □

### *3.2. The projection operator $P_S$*

Let $D$ be an open subset of $\Omega$ associated with a simplicial conforming triangulation $\mathcal{T}_D$ and let $S_1(D;\mathcal{T}_D)$ be the corresponding P1 conforming finite element space with homogeneous boundary conditions on $\partial\Omega \cap \partial D$. For each vertex $p \in \mathcal{P}_D$, we define a domain $D_p$ by $\overline{D}_p := \{T \in \mathcal{T}_D \,|\, p \text{ a vertex of } T\}$ and denote the number of elements contained in $D_p$ by $n_p \le n_{\max} < \infty$.

We will use a projection $P_{S;D} : H^1_{0;\partial\Omega}(D) \to S_1(D;\mathcal{T}_D)$, with the following properties:

(S1) $P_{S;D}v = v$, $v \in S_1(D;\mathcal{T}_D)$,
(S2) $P_{S;D}v(p)$ is uniquely defined by $v|_{\overline{D}_p}$,
(S3) $\|v - P_{S;D}v\|^2_{0;e} \le C_S \frac{h_e}{\alpha_e} |\!|\!| v |\!|\!|^2_{D_e}$ where $D_e := \bigcup_{1\le i\le 2} D_{p_i}$ and $p_i$, $1 \le i \le 2$, are the vertices of $e$,
(S4) $\|v - P_{S;D}v\|^2_{0;T} \le C_S \frac{h_T^2}{\alpha_T} |\!|\!| v |\!|\!|^2_{D_T}$ where $D_T := \bigcup_{1\le i\le 3} D_{p_i}$ and $p_i$, $1 \le i \le 3$, are the vertices of $T$,
(S5) $|\!|\!| P_{S;D}v |\!|\!|^2_T \le C_S |\!|\!| v |\!|\!|^2_{D_T}$ ,

where the constant $C_S$ depends only on the shape regularity of $\mathcal{T}_D$ and the local ratio of the smallest and largest eigenvalues of $a$.

We then can define the global operator $P_S$ by $P_S := \sum_{i=1}^K P_{S;\Omega_i}$ and get a constant in (S3)-(S5) which is independent of $T \in \mathcal{T}_h$. Note that the

well-known interpolation operator of Clément [24] satisfies (S2)-(S5) but not (S1).

*Example.* There are several possibilities to define the operator $P_{S;D}$. The following projection operator $P_{S;D}$ is a simple modification of the operator proposed in [37] (see also [35]): $P_{S;D}v \in S_1(D;\mathcal{T}_D)$ is uniquely determined by its values at the vertices $p$ of the triangulation $\mathcal{T}_D$. They are given by

$$P_{S;D}v(p) := \begin{cases} \frac{1}{n_p} \sum\limits_{T \subset \overline{D}_p} \int\limits_T v\psi_{p;T}\,dx, & p \in D, \\ \frac{1}{2} \sum\limits_{\substack{e \subset \partial D_p \\ p \text{ a vertex of } e}} \int\limits_e v\psi_{p;e}\,d\sigma, & p \in \partial D \setminus \partial\Omega, \\ 0, & p \in \partial D \cap \partial\Omega \end{cases}$$

where $\psi_{p;T}$ and $\psi_{p;e}$ are the dual basis functions of the local nodal basis function $\phi_{p;T}$ in the sense that

$$\int\limits_T \phi_{p_j;T}\,\psi_{p_i;T}\,dx = \delta_{ij}, \quad \int\limits_e \phi_{p_j;T}\,\psi_{p_i;e}\,d\sigma = \delta_{ij}.$$

In [37], $P_{S;D}$ is defined by $P_{S;D}v(p) = \int_e v\psi_{p;e}\,d\sigma$ where $e$ is an arbitrary edge containing the vertex $p$. We note that $\int_e v\psi_{p;e}\,d\sigma$ can be replaced by $\int_T v\psi_{p;T}\,dx$ where $T$ is an arbitrary element containing the vertex $p$ if no boundary condition has to be preserved. Here, we take the average of all possible elements.

### *3.3. Local a posteriori error estimator*

Our introduction of the a posteriori error estimator is based on duality techniques applied to the residual. Using the same arguments as in the conforming setting [40], we evaluate the residual as a continuous linear functional. We obtain from (3.1) for $v \in \prod_{i=1}^k H^1(\Omega_i)$

$$a\,(u - u_{\mathrm{M}}, v) = (f - Lu_{\mathrm{M}}, v)_0 - b\,(\lambda, v) - \sum_{T \in \mathcal{T}_h} \int\limits_{\partial T} a\nabla u_{\mathrm{M}} \boldsymbol{n} v\,d\sigma,$$

(3.3)

where $L$ is applied elementwise to $u_{\mathrm{M}}$. Using the definition of $P_S$ and (2.2), we get

$$a\,(u - u_{\mathrm{M}}, P_S v) = b\,(\lambda_{\mathrm{M}} - \lambda, P_S v)\,, \quad v \in \prod_{i=1}^K H^1(\Omega_i). \tag{3.4}$$

Using (3.3) and (3.4), the variational problem can be written as

$$a\left(u-u_{\mathrm{M}},v\right)=\left(f-Lu_{\mathrm{M}},v-P_Sv\right)_0-b\left(\lambda,v\right)\\ -\sum_{T\in\mathcal{T}_h}\int_{\partial T}a\nabla u_{\mathrm{M}}\boldsymbol{n}(v-P_Sv)\,d\sigma+b\left(\lambda_{\mathrm{M}},P_Sv\right).$$

For $v\in H_0^1(\Omega)+X_h(\Omega)$, we end up with

$$\begin{aligned}a\left(u-u_{\mathrm{M}},v\right)\leq&\sum_{T\in\mathcal{T}_h}\|f-Lu_{\mathrm{M}}\|_{0;T}\|v-P_Sv\|_{0;T}\\&+\sum_{e\in\mathcal{E}_h\setminus\mathcal{S}}\|\left[a\nabla u_{\mathrm{M}}\boldsymbol{n}_e\right]_J\|_{0;e}\|\left[v-P_Sv\right]_A\|_{0;e}\\&+\sum_{e\in\mathcal{E}_h\cap\mathcal{S}}\|\lambda_{\mathrm{M}}-a\nabla u_{\mathrm{M}}\boldsymbol{n}_{ij}|_{T_e}\|_{0;e}\|(v-P_Sv)|_{T_e}\|_{0;e}\\&+\inf_{\mu\in W_h(\mathcal{S})}|b\left(\mu-\lambda,v\right)|.\end{aligned}$$

By means of the saturation assumption (3.2), (S3)-(S4), and choosing $v=u-u_{\mathrm{M}}$, we obtain

$$\begin{aligned}|\!|\!|u-u_{\mathrm{M}}|\!|\!|^2\leq\tilde{C}_{\mathrm{M}}\Bigg(&\|f-Lu_{\mathrm{M}}\|_{\mathcal{T}_h}^2+\sum_{e\in\mathcal{E}_h\setminus\mathcal{S}}\frac{h_e}{\alpha_e}\|\left[a\nabla u_{\mathrm{M}}\boldsymbol{n}_e\right]_J\|_{0;e}^2\\&+\sum_{e\in\mathcal{E}_{\mathrm{L}}}\frac{h_e}{\alpha_e}\|a\nabla u_{\mathrm{M}}\boldsymbol{n}_{ij}-\lambda_{\mathrm{M}}\|_{0;e}^2\\&+\sum_{e\in\mathcal{E}_{\mathrm{M}}}\frac{h_e}{\alpha_e}\|a\nabla u_{\mathrm{M}}\boldsymbol{n}_{ij}-\lambda_{\mathrm{M}}\|_{0;e}^2+\|\left[u_{\mathrm{M}}\right]_J\|_{\mathrm{L}^{-1}}^2\Bigg)\end{aligned}\tag{3.5}$$

where the weighted norm $\|\cdot\|_{\mathcal{T}_h}$ is defined as $\|v\|_{\mathcal{T}_h}^2:=\sum_{T\in\mathcal{T}_h}\frac{h_T^2}{\alpha_T}\|v\|_{0;T}^2$.

These preliminary computations motivate the definition of the local a posteriori residual based error estimator $\eta_{\mathrm{R}}:=\sum_{T\in\mathcal{T}_h}\eta_{\mathrm{R};T}^2$, where

$$\begin{aligned}\eta_{\mathrm{R;T}}^2:=&\frac{h_T^2}{\alpha_T}\|\Pi_1f-Lu_{\mathrm{M}}\|_{0;T}^2+\frac{2\alpha_{T_1}\alpha_{T_2}}{(\alpha_{T_2}+\alpha_{T_1})^2}\sum_{e\subset\partial T\setminus\mathcal{S}}\frac{h_e}{\alpha_T}\|\left[a\nabla u_{\mathrm{M}}\boldsymbol{n}_e\right]_J\|_{0;e}^2\\&+\sum_{e\subset\partial T\cap\mathcal{S}}\frac{h_e}{\alpha_e}\|a\nabla u_{\mathrm{M}}\boldsymbol{n}_{ij}|_T-\lambda_{\mathrm{M}}\|_{0;e}^2\\&+\sum_{e\subset\partial T\cap\mathcal{E}_{\mathrm{L}}}\frac{\alpha_e}{h_e}\|\left[u_{\mathrm{M}}\right]_J\|_{0;e}^2,\quad T\in\mathcal{T}_h.\end{aligned}$$

Here $e=\partial T_1\cap\partial T_2$ for $e\in\mathcal{E}_h\setminus\mathcal{S}$. The first two terms of the error estimator are exactly the same as in the conforming setting while the third and fourth terms are associated with the skeleton. In particular, the third term is connected with the Neumann boundary values at the interior subdomains boundaries. The fourth part reflects the nonconformity of the finite element solution and only comes into play on the non-mortar side.

For the rest of this section, we assume that there exists a constant $C_{\mathcal{S}}$, independent of the refinement level, such that

$$\frac{h_{e_{\mathrm{M}}}^3}{a_{e_{\mathrm{M}}}} \frac{a_{e_{\mathrm{L}}}}{h_{e_{\mathrm{L}}}^3} \leq C_{\mathcal{S}}, \quad e_{\mathrm{L}} \in \mathcal{E}_{\mathrm{L}},\ e_{\mathrm{M}} \in \mathcal{E}_{\mathrm{M}} \text{ and } e_{\mathrm{L}} \cap e_{\mathrm{M}} \neq \emptyset. \tag{3.6}$$

Within the adaptive refinement process, we should make sure that $C_{\mathcal{S}}$ is reasonable bounded.

**Theorem 3.2** *Under the weak saturation assumption (3.2) and (3.6) there exist constants $c_{\mathrm{res}}$, $C_{\mathrm{res}} > 0$ and $c_{\mathrm{high}}$, $C_{\mathrm{high}} > 0$ independent of the refinement level, such that*

$$\begin{aligned} c_{\mathrm{res}}\eta_{\mathrm{R}}^2 - c_{\mathrm{high}}\|f - \Pi_1 f\|_{\mathcal{T}_h}^2 &\leq |||u - u_{\mathrm{M}}|||^2 \\ &\leq C_{\mathrm{res}}\eta_{\mathrm{R}}^2 + C_{\mathrm{high}}\|f - \Pi_1 f\|_{\mathcal{T}_h}^2. \end{aligned} \tag{3.7}$$

*Proof.* The upper bound is an immediate consequence of (3.5) and of the local definition of the a posteriori error estimator.

To establish the lower bound for $|||u - u_{\mathrm{M}}|||$, we have to consider the four different parts of the error estimator separately. Using the same arguments as in the conforming setting [40], we obtain upper bounds for the first two parts of the error estimator. This can be achieved by using cubic bubble functions $\Phi_T$ for $T \in \mathcal{T}_h$ and quadratic bubble functions $\Phi_e$ for $e \in \mathcal{E}_h \setminus \mathcal{S}$ (see [40]). The proof that this works is well known and is therefore omitted. There remains to establish upper bounds for the third and fourth part of the error estimator. On the non-mortar sides $(a\nabla u_{\mathrm{M}} \boldsymbol{n}_{ij}|_{T_e} - \lambda_{\mathrm{M}})$, restricted on $e \in \mathcal{E}_{\mathrm{L}}$, is a linear function (see the left part of Fig. 3.1).

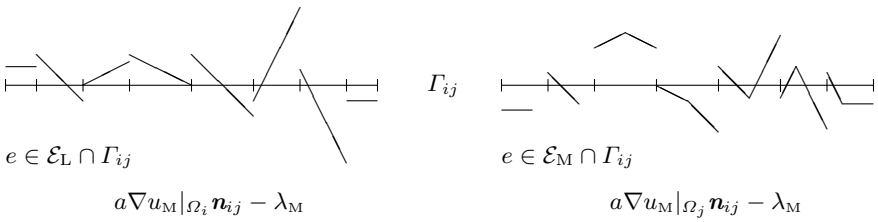


**Fig. 3.1.** $\nabla u_{\mathrm{M}} \boldsymbol{n}_{ij} - \lambda_{\mathrm{M}}$ restricted on $\Gamma_{ij}$

Using quadratic bubble functions $\Phi_e$, $e \in \mathcal{E}_{\mathrm{L}} \cap \Gamma_{ij}$ living in the non-mortar subdomains $\Omega_i$, we obtain for $e \subset \partial T$

$$\begin{aligned} c\|a\nabla u_{\mathrm{M}} \boldsymbol{n}_{ij}|_T - \lambda_{\mathrm{M}}\|_{0;e}^2 &\leq \int_e \left(a\nabla u_{\mathrm{M}} \boldsymbol{n}_{ij}|_T - \lambda_{\mathrm{M}}\right)^2 \Phi_e \, d\sigma \\ &= a\left(u_{\mathrm{M}} - u, \left(a\nabla u_{\mathrm{M}} \boldsymbol{n}_{ij}|_T - \lambda_{\mathrm{M}}\right)^{\mathrm{T}} \Phi_e\right) \end{aligned}$$

$$
\begin{aligned}
&+(f - Lu_{\mathrm{M}}, (\lambda_{\mathrm{M}} - a\nabla u_{\mathrm{M}} \boldsymbol{n}_{ij}|_T)^{\mathrm{T}} \Phi_e)_{0;T} \\
&-b\,(\lambda - \lambda_{\mathrm{M}}, (a\nabla u_{\mathrm{M}} \boldsymbol{n}_{ij}|_T - \lambda_{\mathrm{M}})\,\Phi_e) \\
&\leq C \left( \left( \frac{\alpha_e}{h_e} \right)^{1/2} |\!|\!| u - u_{\mathrm{M}} |\!|\!|_T + h_T^{1/2} \|f - Lu_{\mathrm{M}}\|_{0;T} + \|\lambda - \lambda_{\mathrm{M}}\|_{0;e} \right) \\
&\times \|a\nabla u_{\mathrm{M}} \boldsymbol{n}_{ij}|_T - \lambda_{\mathrm{M}}\|_{0;e}.
\end{aligned}
$$

Here, $(a\nabla u_{\mathrm{M}} \boldsymbol{n}_{ij}|_T - \lambda_{\mathrm{M}})^T$ is a linear function on $T$ with trace $a\nabla u_{\mathrm{M}} \boldsymbol{n}_{ij}|_T - \lambda_{\mathrm{M}}$ on $e$. Summing over all $e \in \mathcal{E}_{\mathrm{L}}$ and using Lemma 3.1, the following upper bound holds:

$$
\sum_{e \in \mathcal{E}_{\mathrm{L}}} \frac{h_e}{\alpha_e} \|a\nabla u_{\mathrm{M}} \boldsymbol{n}_{ij}|_{T_e} - \lambda_{\mathrm{M}}\|_{0;e}^2 \leq C \left( |\!|\!| u - u_{\mathrm{M}} |\!|\!|^2 + \|f - \Pi_1 f\|_{\mathcal{T}_h}^2 \right).
$$

In contrast to the non-mortar sides, $(a\nabla u_{\mathrm{M}} \boldsymbol{n}_{ij}|_{T_e} - \lambda_{\mathrm{M}})|_e$, $e \in \mathcal{E}_{\mathrm{M}}$ is generally not a linear function on $e$ (see the right part of Fig. 3.1). Thus, the upper bound for

$$
\sum_{e \in \mathcal{E}_{\mathrm{M}}} \frac{h_e}{\alpha_e} \|a\nabla u_{\mathrm{M}} \boldsymbol{n}_{ij}|_{T_e} - \lambda_{\mathrm{M}}\|_{0;e}^2
$$

cannot be established as easily as the previous one. Let $\Pi_{\bar{e}} : L^2(\bar{e}) \longrightarrow P_0(\bar{e})$, be the weighted $L^2$-projection given by

$$
\int_{\bar{e}} \Pi_{\bar{e}} v \phi_{\bar{e}}\, d\sigma = \int_{\bar{e}} v \phi_e\, d\sigma, \quad v \in L^2(\bar{e}).
$$

Then, it can be easily seen that

$$
\|v\|_{0;\bar{e}}^2 \leq C(\|\Pi_{\bar{e}} v\|_{0;\bar{e}}^2 + h_{\bar{e}}^2 |v|_{1;\bar{e}}^2), \quad v \in H^1(\bar{e})
$$

holds. Using the same techniques as before, we get

$$
\begin{aligned}
&\|a\nabla u_{\mathrm{M}} \boldsymbol{n}_{ij}|_T - \Pi_{\bar{e}} \lambda_{\mathrm{M}}\|_{0;\bar{e}} \\
&\leq C \left( \left( \frac{\alpha_{\bar{e}}}{h_{\bar{e}}} \right)^{1/2} |\!|\!| u - u_{\mathrm{M}} |\!|\!|_T + h_T^{1/2} \|f - Lu_{\mathrm{M}}\|_{0;T} + \|\lambda - \lambda_{\mathrm{M}}\|_{0;\bar{e}} \right)
\end{aligned}
$$

for $\bar{e} \in \mathcal{E}_{\mathrm{M}} \cap \partial T \cap \partial \Gamma_{ij}$. In addition, we obtain

$$
h_e |\lambda_{\mathrm{M}}|_{1;e} \leq \|a\nabla u_{\mathrm{M}} \boldsymbol{n}_{ij}|_{T_e} - \lambda_{\mathrm{M}}\|_{0;e}, \quad e \in \mathcal{E}_{\mathrm{L}}
$$

and thus

$$
\sum_{\bar{e} \in \mathcal{E}_{\mathrm{M}}} \frac{h_{\bar{e}}}{\alpha_{\bar{e}}} \|a\nabla u_{\mathrm{M}} \boldsymbol{n}_{ij}|_{T_{\bar{e}}} - \lambda_{\mathrm{M}}\|_{0;\bar{e}}^2 \leq C_{\mathrm{M}} \left( |\!|\!| u - u_{\mathrm{M}} |\!|\!|^2 + \|f - \Pi_1 f\|_{\mathcal{T}_h}^2 \right).
$$

To control the last term of the error estimator, we consider the $L^2$-orthogonal projection operator $P_{ij} : L^2(\Gamma_{ij}) \longrightarrow W(\Gamma_{ij}; \mathcal{T}_{h_i})$ defined by

$$\int_{\Gamma_{ij}} P_{ij} v \mu \, d\sigma = \int_{\Gamma_{ij}} v \mu \, d\sigma, \quad \mu \in W(\Gamma_{ij}; \mathcal{T}_{h_i}).$$

Then, there exits a constant $C_\Gamma$ independent of $i$ and $j$, $1 \leq i \leq K$, $j \in \mathcal{M}(i)$, such that

$$\sum_{e \in \mathcal{E}_{\mathrm{L}} \cap \Gamma_{ij}} \frac{1}{h_e} \| v - P_{ij} v \|^2_{0;e} \leq C_\Gamma |v|^2_{1/2;\Gamma_{ij}}, \quad v \in H^{1/2}(\Gamma_{ij}). \tag{3.8}$$

(3.8) can be proved by using a locally defined quasi-interpolant with this property and by taking the stability property of $P_{ij}$, with respect to the weighted $L^2$-norm $\| \cdot \|_{\mathrm{L}^{-1}}$, into account. By means of (3.8) and $P_{ij}(u_{\mathrm{M}}|_{\Omega_i}) = P_{ij}(u_{\mathrm{M}}|_{\Omega_j})$, we get

$$\begin{aligned}
&\sum_{e \in \mathcal{E}_{\mathrm{L}}} \frac{\alpha_e}{h_e} \| \, [u_{\mathrm{M}}]_J \, \|^2_{0;e} = \sum_{e \in \mathcal{E}_{\mathrm{L}}} \frac{\alpha_e}{h_e} \| \, [u_{\mathrm{M}} - u - P_{ij}(u_{\mathrm{M}} - u)]_J \, \|^2_{0;e} \\
&\leq 2 C_\Gamma \sum_{i=1}^{K} \sum_{j \in \mathcal{M}(i)} \left( \alpha_{\Omega_i} |u_{\mathrm{M}}|_{\Omega_i} - u|^2_{1/2;\Gamma_{ij}} + \alpha_{\Omega_j} |u_{\mathrm{M}}|_{\Omega_j} - u|^2_{1/2;\Gamma_{ij}} \right) \\
&\leq \hat{C}_\Gamma |\!|\!| u - u_{\mathrm{M}} |\!|\!|^2.
\end{aligned}$$

□

*Remark 3.1.* The constant $C_{\mathrm{M}}$ depends on $C_{\mathcal{S}}$ (see definition (3.6)), which should be kept reasonable small, as well as on the variation of the eigenvalues of $a$ across the skeleton. The constant $\hat{C}_\Gamma$ depends on the variation of the eigenvalues of $a$ on the subdomains. Therefore, the decomposition into subdomains should preferable be done taking the matrix-valued function $a$ into account. If we examine the constants that depend on the eigenvalues of $a$ in more detail, it turns out that they are better in the case when the non-mortar side is associated with the smaller coefficient $a$. This can be also seen by a careful a priori analysis and is supported by our numerical results. In the numerical results, it can be very often observed that the local ratio $h^4_{e_{\mathrm{L}}}/h^4_{e_{\mathrm{M}}}$ tends asymptotically to $a_{e_{\mathrm{L}}}/a_{e_{\mathrm{M}}}$. Starting with a quasi-uniform global discretization and taking the non-mortar side where the coefficient is smaller yield a constant $C_{\mathcal{S}}$ of order one.

*Remark 3.2.* In general, the term $\| f - \Pi_1 f \|^2_{\mathcal{T}_h}$ is of higher order and can be neglected. This also holds true if we replace $\Pi_1 f$ by $\Pi_0 f$.

## 4. Crouzeix–Raviart discretization

We now consider a nonconforming discretization with Crouzeix-Raviart finite elements of lowest order. This method is closely related to mixed finite element discretizations [7]. A residual based a posteriori error estimator for Crouzeix-Raviart finite elements has been introduced and analyzed in our earlier work [41]. There a weak saturation assumption was used to prove upper and lower bounds for the true error in the energy norm. Here, we will prove the efficiency and reliability of the error estimator without any saturation assumption. A similar result can be found in [22,25]. There, the introduction of a residual based error estimator is based on a Helmholtz type decomposition of the gradient of the error. The results in [22,25] are restricted to the special case of a vanishing zero order term $b$. Here, we consider the more general case $b \geq 0$.

### *4.1. Variational problem*

We consider a simplicial triangulation $\mathcal{T}_l$ of $\Omega$ obtained from an initial coarse triangulation $\mathcal{T}_0$ by the adaptive refinement process of Bank et al. [11]. The sets of vertices and edges of $\mathcal{T}_l$ are denoted by $\mathcal{P}_l$ and $\mathcal{E}_l$, respectively. We assume that each edge $e \in \mathcal{E}_l$ is either contained in the interior of $\Omega$ or that $e \subset \partial\Omega$. Let $\mathcal{E}_l^{\mathrm{B}} \subset \mathcal{E}_l$ stand for the set of all edges on the boundary of $\Omega$, and let $m_e$ denote the midpoint for every edge $e \in \mathcal{E}_l$: There exist $T_i$ and $T_{\mathrm{o}}$ with $\partial T_i \cap \partial T_{\mathrm{o}} = e$, if $e \in \mathcal{E}_l \setminus \mathcal{E}_l^{\mathrm{B}}$ and a $T_i$ with $e \subset \partial T_i \cap \partial\Omega$, if $e \in \mathcal{E}_l^{\mathrm{B}}$. The subdomain $D_e$ is given by $\overline{D}_e := T_i \cup T_{\mathrm{o}}$ and $\overline{D}_e := T_i$ if $e \in \mathcal{E}_l \setminus \mathcal{E}_l^{\mathrm{B}}$ and $e \in \mathcal{E}_l^{\mathrm{B}}$, respectively. The unit outer normal on $T_i$ is denoted by $\boldsymbol{n}_e$. The orientation of the vector $\boldsymbol{n}_e$ is arbitrary but fixed. We recall that the largest eigenvalue of $a$ restricted on $T$ is denoted by $\alpha_T$, and $\alpha_e$ is defined by $\alpha_e := \frac{1}{2}(\alpha_{T_i} + \alpha_{T_{\mathrm{o}}})$ if $e \in \mathcal{E}_l \setminus \mathcal{E}_l^{\mathrm{B}}$ and by $\alpha_e := \alpha_{T_i}$ if $e \in \mathcal{E}_l^{\mathrm{B}}$. Finally, $h_e$ and $h_T$ denote the length of the edge $e$ and the diameter of the element $T$, respectively.

The Crouzeix-Raviart space of lowest order associated with the triangulation $\mathcal{T}_l$, $l \geq 0$, is defined by

$$\begin{aligned} CR(\Omega;\mathcal{T}_l) := \Big\{ & v \in L^2(\Omega) \mid v|_T \in P_1(T),\ T \in \mathcal{T}_l, \\ & v(m_e)|_{T_i} = 0,\ e \in \mathcal{E}_l^{\mathrm{B}} \\ & v|_{T_i}(m_e) = v|_{T_{\mathrm{o}}}(m_e),\ e \in \mathcal{E}_l \setminus \mathcal{E}_l^{\mathrm{B}} \Big\}. \end{aligned}$$

We can then consider the discrete variational problem: Find $u_{\mathrm{CR}} \in CR(\Omega; \mathcal{T}_l)$ such that

$$a_{\mathrm{CR}}(u_{\mathrm{CR}}, v) = (f, v)_0, \quad v \in CR(\Omega;\mathcal{T}_l) \tag{4.1}$$

where the bilinear form $a_{\mathrm{CR}}(\cdot,\cdot)$ is given by $a_{\mathrm{CR}}(v,w) := \sum_{T\in\mathcal{T}_l}\int_T a\nabla v \times \nabla w\,dx + \int_\Omega bvw\,dx$. The discrete energy norm is denoted by $|||v|||^2 := a_{\mathrm{CR}}(v,v)$. The variational problem (4.1) is solved iteratively, and we let $\hat{u}_{\mathrm{CR}}$ stand for the available approximate solution so obtained.

### *4.2. Nonconformity of Crouzeix-Raviart finite elements*

As we have seen in Sect. 3, we have to take the jump of the nonconforming finite element solution into account in the definition of a residual based error estimator. In a first step, we decompose the nonconforming space locally into a conforming space and a nonconforming surplus space.

For each $p \in \mathcal{P}_l$, we consider the subdomain $D_p$ which contains all elements having the vertex $p$ in common, $\overline{D}_p := \bigcup\{T \in \mathcal{T}_l \mid\ p \text{ a vertex of } T\}$, and we denote by $n_p \le n_{\max} < \infty$ the number of elements contained in $D_p$ (see Fig. 4.1).

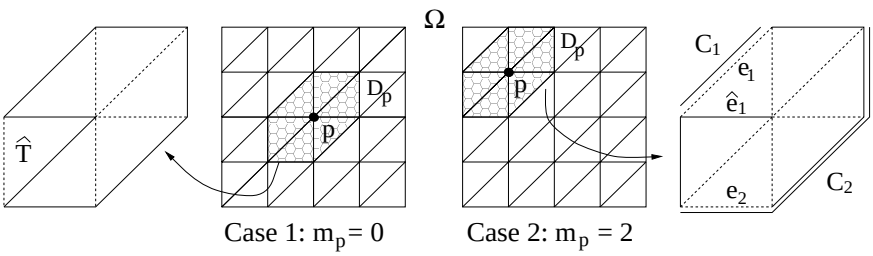


**Fig. 4.1.** Definition of $D_p$ and $\tilde{\mathcal{E}}_p$ (edges marked by dashed lines)

We now focus on the splitting of the nonconforming space $CR(D_p;\mathcal{T}_l)$ restricted to $D_p$ given by

$$CR(D_p;\mathcal{T}_l) := \{v \in L^2(D_p) |\ v = w|_{D_p},\ w \in CR(\Omega;\mathcal{T}_l)\}.$$

Let $S(D_p;\mathcal{T}_l)$ be the space of conforming P1 finite elements on $D_p$ with homogeneous boundary conditions on $\partial D_p \cap \partial\Omega$. To obtain a direct decomposition of $CR(D_p;\mathcal{T}_l)$ into $S(D_p;\mathcal{T}_l)$ and a nonconforming surplus ansatz space $N(D_p;\mathcal{T}_l)$, we have to distinguish between several cases. Let $\mathcal{E}_p^{\mathrm{I}}$ be the set of all edges $e \in \mathcal{E}_l$ contained in the interior of $D_p$ and let $\mathcal{E}_p^{\mathrm{B}}$ be the set of edges on the boundary $\partial D_p$. Two different cases have to be considered. We first focus on the case that $\partial D_p$ does not contain any boundary vertex of $\Omega$ (see case 1 of Fig. 4.1). If the number $n_p$ of elements of $D_p$ is odd, let

$$\tilde{\mathcal{E}}_p := \{e \in \mathcal{E}_p^{\mathrm{I}} |\ \ e \neq \hat{e}\}$$

where $\hat{e}$ is a fixed but arbitrary element of $\mathcal{E}_p^{\mathrm{I}}$. If $n_p$ is even, let

$$\tilde{\mathcal{E}}_p := \{e \in \mathcal{E}_p^{\mathrm{I}} |\ \ e \not\subset \partial\hat{T}\} \cup \{e \in \mathcal{E}_p^{\mathrm{B}} |\ \ e \subset \partial\hat{T}\}$$

where $\hat{T}$ is a fixed but arbitrary element of $D_p$ (see left part of Fig. 4.1).

In the second case, $\partial D_p$ contains at least one vertex on the boundary of $\Omega$ (see case 2 of Fig. 4.1). For each connected set $C_i$, $0 \le i \le m_p$, of boundary edges of $D_p$ which are in the interior of $\Omega$, we fix one $e_i$ such that $e_i \subset C_i \cap \mathcal{E}_p^{\mathrm{B}}$ contains an endpoint of $C_i$. Note that $m_p = 0$ if and only if $D_p = \Omega$. Now, $\tilde{\mathcal{E}}_p$ is given by

$$\tilde{\mathcal{E}}_p := \{e \in \mathcal{E}_p^{\mathrm{I}}\} \cup \bigcup_{i=1}^{m_p} \{e_i\},$$

if $p \in \partial\Omega$, and by

$$\tilde{\mathcal{E}}_p := \{e \in \mathcal{E}_p^{\mathrm{I}} |\ \ e \neq \hat{e}_1\} \cup \bigcup_{i=1}^{m_p} \{e_i\},$$

if $p \in \Omega$, where $\hat{e}_1 \in \mathcal{E}_p^{\mathrm{I}}$, and $\hat{e}_1$ and $e_1$ are edges of one triangle $\hat{T} \subset D_p$ if $m_p \ge 1$ (see right part of Fig. 4.1), and $\hat{e}_1$ is arbitrary if $m_p = 0$.
The definition of the nonconforming surplus $N(D_p; \mathcal{T}_l)$ is now given by

$$N(D_p; \mathcal{T}_l) := \Big\{ v \in L^2(D_p) |\ \ v = \sum_{e \in \tilde{\mathcal{E}}_p} \omega_e \Phi_e|_{D_p},\ \omega_e \in \mathbb{R} \Big\},$$

where $\Phi_e$ denotes the standard nonconforming nodal basis function associated with the edge $e$.

**Lemma 4.1** *For each $p \in \mathcal{P}_l$, the nonconforming space $CR(D_p; \mathcal{T}_l)$ can be decomposed as a direct sum*

$$CR(D_p; \mathcal{T}_l) = S(D_p; \mathcal{T}_l) \oplus N(D_p; \mathcal{T}_l).$$

*Proof.* We formally set $m_p = 0$ in the case that $\partial D_p$ does not contain any boundary vertex of $\Omega$. Then, $\dim CR(D_p; \mathcal{T}_l) = \#\mathcal{E}_p^{\mathrm{B}} + \#\mathcal{E}_p^{\mathrm{I}} - \#(\mathcal{E}_p^{\mathrm{B}} \cap \mathcal{E}_l^{\mathrm{B}})$, $\dim S(D_p; \mathcal{T}_l) = \#\mathcal{E}_p^{\mathrm{B}} + 1 - \delta_{p;\partial\Omega} - \#(\mathcal{E}_p^{\mathrm{B}} \cap \mathcal{E}_l^{\mathrm{B}}) - m_p$ and $\dim N(D_p; \mathcal{T}_l) = \#\mathcal{E}_p^{\mathrm{I}} - 1 + \delta_{p;\partial\Omega} + m_p$, where $\delta_{p;\partial\Omega} = 0$ if $p \in \Omega$, and $\delta_{p;\partial\Omega} = 1$ if $p \in \partial\Omega$. Thus, we get

$$\dim CR(D_p; \mathcal{T}_l) = \dim S(D_p; \mathcal{T}_l) + \dim N(D_p; \mathcal{T}_l). \tag{4.2}$$

In a next step, we show that

$$S(D_p; \mathcal{T}_l) \cap N(D_p; \mathcal{T}_l) = \{0\}. \tag{4.3}$$

Let $v \in S(D_p;\mathcal{T}_l) \cap N(D_p;\mathcal{T}_l)$. Then, $v$ is continuous across the interior edges of $D_p$ and zero at the vertices of $\partial D_p \cap \partial\Omega$. In the first case where $\partial D_p$ does not contain any boundary vertex of $\Omega$, $v$ can be written as $v = \sum_{i=1}^{n_p-1} \omega_i \Phi_i|_{D_p}$; the notation is explained in Fig. 4.2.

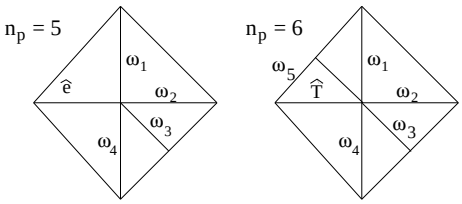


**Fig. 4.2.** Enumeration of the edges $e_i \in \tilde{\mathcal{E}}_p$ (case 1)

We obtain the following conditions

$$\omega_1 = \omega_i + \omega_{i+1} = \omega_{n_p-1}, \quad 1 \le i \le n_p - 2$$

if $n_p$ is odd and

$$\omega_1 = \omega_i + \omega_{i+1} = \omega_{n_p-2} = -\omega_{n_p-1}, \quad 1 \le i \le n_p - 3$$

if $n_p$ is even. It follows that $w_i = 0$, $1 \le i \le n_p - 1$, and thus $v = 0$.

In the second case where $\partial D_p$ contains at least one boundary vertex of $\Omega$, the proof of (4.3) is somewhat more technical but as easy as in the first case. Basically, we have to consider only the case $m_p = 0$; the proof for $m_p \ge 1$ is obtained by induction. The details are omitted. Equation (4.2) together with (4.3) gives the direct decomposition of $CR(D_p;\mathcal{T}_l)$. □

We now use the same type of projection operator $P_S := P_{S;\Omega}$ as in Subsect. 3.2 which should satisfy (S1)-(S5) for $v \in CR(\Omega;\mathcal{T}_l) + H_0^1(\Omega)$. Following the same lines as in [37], the estimates (S1)-(S5) can be easily established for the concrete choice of $P_S$ given in Subsect. 3.2 for $v \in CR(\Omega;\mathcal{T}_l) + H_0^1(\Omega)$.

Let

$$\mathcal{E}_T := \bigcup_{i=1}^{3} \hat{\mathcal{E}}_{p_i}, \quad \hat{\mathcal{E}}_{p_i} := \mathcal{E}_{p_i} \cup \bigcup_{\substack{p \in \partial\Omega \cap \mathcal{P}_l \\ p \text{ a vertex of } e \in \mathcal{E}_{p_i}}} \mathcal{E}_p$$

with $\mathcal{E}_p := \{e \in \mathcal{E}_l,\ p \text{ a vertex of } e\}$, $p \in \mathcal{P}_l$ and $p_i$, $1 \le i \le 3$ are the vertices of $T$. In Fig. 4.3 the edges of $\mathcal{E}_p$, $\hat{\mathcal{E}}_p$ and $\mathcal{E}_T$ are marked by dashed lines.

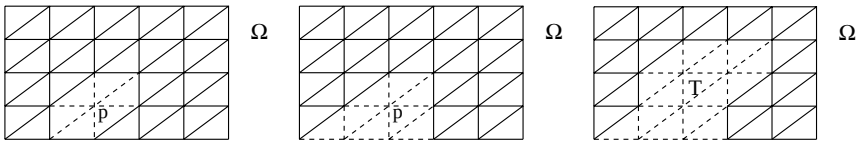


**Fig. 4.3.** The set of edges $\mathcal{E}_p$ (left), $\hat{\mathcal{E}}_p$ (middle) and $\mathcal{E}_T$ (right)

The following lemma provides a measure of the nonconformity of a Crouzeix-Raviart finite element function. In particular, the discontinuity of $v \in CR(\Omega;\mathcal{T}_l)$ across the edges of the triangulation is bounded by $|||w-v|||$ where $w \in H_0^1(\Omega)$ is arbitrary. The definition of the jump depends on the orientation of $\boldsymbol{n}_e$

$$
\begin{aligned}
[v]_J := v|_{T_i} - v|_{T_o}, \quad [v]_A := \frac{1}{2}(v|_{T_i} + v|_{T_o}), \quad & e \in \mathcal{E}_l \setminus \mathcal{E}_l^{\mathrm{B}},\\
[v]_J := v|_{T_i}, \quad [v]_A := \frac{1}{2} v|_{T_i}, \quad & [a\nabla v \boldsymbol{n}_e]_J := 0,\\
[a\nabla v \boldsymbol{n}_e]_A := a\nabla v \boldsymbol{n}_e|_{T_i}, \quad & e \in \mathcal{E}_l^{\mathrm{B}}.
\end{aligned}
$$

**Lemma 4.2** *There exists a constants $0 < \tilde{C}_J$ independent of the refinement level $l$, such that*

$$
|||P_S v - v|||_T^2 \le \tilde{C}_J^2 \sum_{e\in\mathcal{E}_T} \frac{\alpha_e}{h_e} \| [v]_J \|_{0;e}^2, \quad T \in \mathcal{T}_l,\ v \in CR(\Omega;\mathcal{T}_l), \tag{4.4}
$$

*and*

$$
\begin{aligned}
\frac{\alpha_e}{h_e} \| [v]_J \|_{0;e}^2 &\le \tilde{C}_J^2 |||w-v|||_{D_e}^2,\\
& e \in \mathcal{E}_l,\ v \in CR(\Omega;\mathcal{T}_l),\ w \in H_0^1(\Omega).
\end{aligned} \tag{4.5}
$$

*Proof.* We start with the proof of (4.4). On each triangle, an upper bound for the energy norm of the linear function $P_S v - v$ is given by

$$
c|||P_S v - v|||_T^2 \le \alpha_T \sum_{i=1}^{3} (P_S v - v)|_T^2(p_i).
$$

Lemma 4.1 shows that each $v \in CR(\Omega;\mathcal{T}_l)$, restricted to $D_p$, can be uniquely decomposed into

$$
v|_{D_p} = v_S + \tilde{v}_N
$$

where $v_S \in S(D_p;\mathcal{T}_l)$ and $\tilde{v}_N \in N(D_p;\mathcal{T}_l)$. We extend $\tilde{v}_N$ to $v_N \in CR(\Omega;\mathcal{T}_l)$ on $\Omega$ by setting $v_N|_{D_p} = \tilde{v}_N$ and $v_N(m_e) = 0$ for $e \in \mathcal{E}_l \setminus$

$(\mathcal{E}_p^{\mathrm{B}} \cup \mathcal{E}_p^{\mathrm{I}})$. Then, $v_N = \sum_{e \in \tilde{\mathcal{E}}_p} \omega_e \Phi_e$ and $[v_N]_J = [v]_J$ for $e \in \mathcal{E}_p^{\mathrm{I}}$. The continuity of $P_S$, (S1)-(S2), and $(P_S v - v)|_T \in P_1(T)$ yield

$$\begin{aligned}(P_S v - v)|_T^2(p) = (P_S v_N - v_N)|_T^2(p) \;&\le\; C|v_N|_1^2 \;\le\; C \sum_{e \in \tilde{\mathcal{E}}_p} \omega_e^2 \\ &\le C\Big( \sum_{e \in \mathcal{E}_p^{\mathrm{I}}} h_e^{-1} \|[v_N]_J\|_{0;e}^2 + \sum_{\substack{\hat{p} \text{ a vertex of} \\ \partial\Omega \cap \partial D_p}} \sum_{\substack{\hat{T} \subset \overline{D}_p \\ \hat{p} \text{ a vertex of } \hat{T}}} v_N|_{\hat{T}}^2(\hat{p}) \Big) \\ &\le C \sum_{e \in \hat{\mathcal{E}}_p} h_e^{-1} \|[v]_J\|_{0;e}^2.\end{aligned}$$

For the last inequality, we have to use that $v_N|_{\hat{T}}(\hat{p}) = v|_{\hat{T}}(\hat{p})$, $\hat{T} \subset \overline{D}_p$, can be written as a sum of $[v]_J(\hat{p})$, and that the number of terms is bounded by $1/2\, n_{\max} + 1$. Thus, by summing over the three vertices of the element $T$, (4.4) is established.

The second estimate in Lemma 4.2 can be shown easily. Let $\Pi_e$ be the $L^2$-orthogonal projection operator from $L^2(e)$ onto $P_0(e)$. Using $\Pi_e(v|_{T_i}) = \Pi_e(v|_{T_o})$, $e \in \mathcal{E}_l \setminus \mathcal{E}_l^{\mathrm{B}}$ and $\Pi_e(v|_{T_i}) = 0$, $e \in \mathcal{E}_l^{\mathrm{B}}$, we obtain

$$\begin{aligned}h_e^{-1} \|[v]_J\|_{0;e}^2 &= h_e^{-1} \|[w - v]_J\|_{0;e}^2 \\ &\le 2h_e^{-1} \sum_{T \subset \overline{D}_e} \|(w - v - \Pi_e(w - v))|_T\|_{0;e}^2 \\ &\le 2h_e^{-1} \sum_{T \subset \overline{D}_e} \|(w - v - \Pi_0(w - v))|_T\|_{0;e}^2 \\ &\le c \sum_{T \subset \overline{D}_e} |w - v|_{1;T}^2, \quad w \in H_0^1(\Omega),\end{aligned}$$

where $\Pi_0$ is the $L^2$-projection on $P_0(T)$. Thus, (4.5) holds. □

If we use the operator $P_S$ proposed in Subsect. 3.2, we immediately get

$$P_S v(p) = \begin{cases} \frac{1}{n_p} \sum_{T \subset \overline{D}_p} v|_T(p), & p \in \Omega \cap \mathcal{P}_l, \\ 0, & p \in \partial\Omega \cap \mathcal{P}_l. \end{cases}$$

Thus, we obtain

$$\begin{aligned}(v - P_S v)|_T^2(p) = (v|_T - \frac{1}{n_p} \sum_{T' \subset \overline{D}_p} v|_{T'}(p))^2 \\ \le \frac{1}{n_p} \sum_{T' \subset \overline{D}_p} (v|_T - v|_{T'})^2(p) \\ \le C \sum_{\substack{e \in \mathcal{E}_l \\ p \text{ a vertex of } e}} h_e^{-1} \|[v]_J\|_{0;e}^2\end{aligned}$$

for all $p \in \Omega \cap \mathcal{P}_l$ where the constant $C$ depends only on $n_{\max}$. For a boundary vertex, we have the same type of upper bound.

*Remark 4.1.* The estimate (4.4) holds true for each projection operator satisfying (S1)-(S5) and $\tilde{C}_J$ depends only on the constant in (S3)-(S5), the shape regularity of $\mathcal{T}_0$, the local variation of the eigenvalues of $a$ and the local ratio of $a$ and $h^2 b$.

### *4.3. Definition of the residual based error estimator*

As mentioned in Sect. 3, the main difficulty in the construction of an efficient and reliable error estimator is the nonconformity of the space. In general, the available approximation $\hat{u}_{\mathrm{CR}}$, of the solution $u_{\mathrm{CR}}$ of (4.1), is not contained in $H_0^1(\Omega)$, and we have to take the discontinuity of $\hat{u}_{\mathrm{CR}}$ across the edges into account. We assume that the weak solution $u$ is contained in $\prod_{T\in\mathcal{T}_0} H^2(T)$, that the jump of $a\nabla u \boldsymbol{n}_e$ vanishes across the interior edges and that $a$ restricted to $T \in \mathcal{T}_0$ is a polynomial.

It is easy to see that the error $u_e := u - \hat{u}_{\mathrm{CR}}$ satisfies the following defect problem

$$a_{\mathrm{CR}}(u_e, v) = r(v), \quad v \in H_0^1(\Omega) + CR(\Omega; \mathcal{T}_l),$$

where the residual $r(\cdot)$ is defined by

$$\begin{aligned} r(v) := &\int_\Omega f v \, dx + \sum_{e\in\mathcal{E}_l} \int_e [a\nabla u \boldsymbol{n}_e]_A \, [v]_J \, d\sigma \\ &- \sum_{T\in\mathcal{T}_l} \int_T a\nabla \hat{u}_{\mathrm{CR}} \nabla v \, dx - \int_\Omega b\hat{u}_{\mathrm{CR}} v \, dx. \end{aligned}$$

In order to study this error estimator, it is sufficient to consider the residual in detail. Integrating by parts, we obtain

$$\begin{aligned} r(v) = &\sum_{T\in\mathcal{T}_l} \int_T (f - L\hat{u}_{\mathrm{CR}})\, v \, dx + \sum_{e\in\mathcal{E}_l} \int_e [a\nabla(u - \hat{u}_{\mathrm{CR}})\boldsymbol{n}_e]_A \, [v]_J \, d\sigma \\ &- \sum_{e\in\mathcal{E}_l} \int_e [a\nabla \hat{u}_{\mathrm{CR}} \boldsymbol{n}_e]_J \, [v]_A \, d\sigma \end{aligned}$$

where the differential operator $L$ is applied elementwise to $\hat{u}_{\mathrm{CR}}$. The discretization error $u - u_{\mathrm{CR}}$ is orthogonal on $S_1(\Omega; \mathcal{T}_l) = CR(\Omega; \mathcal{T}_l) \cap H_0^1(\Omega)$ with respect to the bilinear form $a_{\mathrm{CR}}(\cdot, \cdot)$. Thus,

$$r(v) = a_{\mathrm{CR}}(u_{\mathrm{CR}} - \hat{u}_{\mathrm{CR}}, v), \quad v \in S_1(\Omega; \mathcal{T}_l).$$

Given that $|||u - \hat{u}_{\rm CR}|||^2 = r(u - \hat{u}_{\rm CR})$, we get

$$\begin{aligned}|||u - \hat{u}_{\rm CR}|||^2 = &\sum_{T\in\mathcal{T}_l}\int_T (f - L\hat{u}_{\rm CR})\,(u - P_S u)\,dx\\ &-\sum_{e\in\mathcal{E}_l}\int_e [a\nabla\hat{u}_{\rm CR}\boldsymbol{n}_e]_J\,[u - P_S u]_A\,d\sigma\\ &+a_{\rm CR}\,(u - \hat{u}_{\rm CR}, P_S\hat{u}_{\rm CR} - \hat{u}_{\rm CR})\\ &+a_{\rm CR}\,(u_{\rm CR} - \hat{u}_{\rm CR}, P_S\,(u - \hat{u}_{\rm CR}))\,.\end{aligned}$$

Taking (S3)-(S5) into account, the following estimate holds

$$\begin{aligned}c|||u - \hat{u}_{\rm CR}|||^2 \le C_S|||u - P_S u|||\,(&|||f - L\hat{u}_{\rm CR}|||_{\mathcal{T}_l} + |||[a\nabla\hat{u}_{\rm CR}\boldsymbol{n}_e]_J|||_{\mathcal{E}_l})\\ &+|||u - \hat{u}_{\rm CR}|||\,(C_S|||u_{\rm CR} - \hat{u}_{\rm CR}||| + |||P_S\hat{u}_{\rm CR} - \hat{u}_{\rm CR}|||)\,,\end{aligned}\tag{4.6}$$

where the weighted norms $|||\cdot|||_{\mathcal{T}_l}$ and $|||\cdot|||_{\mathcal{E}_l}$ are defined by

$$|||v|||^2_{\mathcal{T}_l} := \sum_{T\in\mathcal{T}_l}\frac{h_T^2}{\alpha_T}\|v\|^2_{0;T},\quad |||v|||^2_{\mathcal{E}_l} := \sum_{e\in\mathcal{E}_l}\frac{h_e}{\alpha_e}\|v\|^2_{0;e}.$$

The triangle inequality and the continuity of $P_S$ yield

$$|||u - P_S u||| \le (1 + C_S)|||u - \hat{u}_{\rm CR}||| + |||P_S\hat{u}_{\rm CR} - \hat{u}_{\rm CR}|||.$$

To establish an upper bound for $|||u - \hat{u}_{\rm CR}|||$, there remains to consider $|||P_S\hat{u}_{\rm CR} - \hat{u}_{\rm CR}|||$ in more detail. We note that local estimates are given in Lemma 4.2. Due to $n_p \le n_{\max}$, we obtain the corresponding global estimates from (4.4) and (4.5) with a constant $C_J$. Combining Lemma 4.2 and (4.6), we finally get an upper bound of the true error in the energy norm

$$\begin{aligned}c_{err}|||u - \hat{u}_{\rm CR}||| \le &|||f - L\hat{u}_{\rm CR}|||_{\mathcal{T}_l} + |||[a\nabla\hat{u}_{\rm CR}\boldsymbol{n}_e]_J|||_{\mathcal{E}_l}\\ &+\left(\sum_{e\in\mathcal{E}_l}\frac{\alpha_e}{h_e}\|\,[\hat{u}_{\rm CR}]_J\,\|^2_{0;e}\right)^{1/2} + |||u_{\rm CR} - \hat{u}_{\rm CR}|||.\end{aligned}\tag{4.7}$$

The first three terms of the right hand side in (4.7) are independent of the weak solution $u$ and can be evaluated easily. The fourth term is the iteration error and has to be controlled in the iterative solution process.

These considerations lead to the definition of a residual based a posteriori error estimator $\eta_R^2 := \sum_{T\in\mathcal{T}_l}\eta^2_{{\rm R};T}$ with

$$\begin{aligned}\eta^2_{{\rm R};T} := &\frac{h_T^2}{\alpha_T}\|\Pi_1 f - L\hat{u}_{\rm CR}\|^2_{0;T} + \sum_{i=1}^{3}\hat{w}_i\frac{h_{e_i}}{\alpha_T}\int_{e_i}[a\nabla\hat{u}_{\rm CR}\boldsymbol{n}_e]_J^2\,d\sigma\\ &+\sum_{i=1}^{3}w_i\frac{\alpha_T}{h_{e_i}}\int_{e_i}[\hat{u}_{\rm CR}]_J^2\,d\sigma,\end{aligned}$$

where $e_i$, $1 \leq i \leq 3$, denote the edges of the element $T$. The weights $w_i$ and $\hat{w}_i$ are given by $w_i = \frac{1}{2}$, $\hat{w}_i = \frac{2\alpha_{T_\mathrm{o}}\alpha_{T_i}}{(\alpha_{T_\mathrm{o}}+\alpha_{T_i})^2}$ if $e_i \in \mathcal{E}_l \setminus \mathcal{E}_l^{\mathrm{B}}$, $T_\mathrm{i} \cap T_\mathrm{o} = e_i$, and by $w_i = \hat{w}_i = 1$ if $e_i \in \mathcal{E}_l^{\mathrm{B}}$.

**Theorem 4.3** *There exist constants $0 < c_\mathrm{R} \leq C_\mathrm{R}$ and $\gamma_\mathrm{R} > 0$, independent of the refinement level $l \geq 1$, such that*

$$
\begin{aligned}
&|||u - \hat{u}_{\mathrm{CR}}||| \leq C_\mathrm{R}\left(\eta_\mathrm{R} + |||f - \Pi_1 f|||_{\mathcal{T}_l} + |||\hat{u}_{\mathrm{CR}} - u_{\mathrm{CR}}|||\right), \\
&|||u - \hat{u}_{\mathrm{CR}}||| \geq c_\mathrm{R}\left(\eta_\mathrm{R} - \gamma_\mathrm{R}|||f - \Pi_1 f|||_{\mathcal{T}_l}\right).
\end{aligned} \tag{4.8}
$$

*Proof.* The upper bound is an easy consequence of the triangle inequality, (4.7), and the definition of the error estimator.

To prove the lower bound, we have to consider the three parts of the error estimator separately. Upper bounds of $\|\Pi_1 f - L\hat{u}_{\mathrm{CR}}\|_{0;T}$ and $\|[a\nabla\hat{u}_{\mathrm{CR}}\boldsymbol{n}_e]_J\|_{0;e}$ follow exactly as in the conforming setting [40]. The third term $|||[\hat{u}_{\mathrm{CR}}]_J|||_{0;\mathcal{E}_l^{-1}}$ is already considered in Lemma 4.2. Estimate (4.5) even guarantees a local upper bound for $|||[\hat{u}_{\mathrm{CR}}]_J|||_{0;\mathcal{E}_l^{-1}}$. □

A careful analysis guarantees not only global estimates, but also

$$
\begin{aligned}
&\eta_{\mathrm{R};T}^2 \\
&\leq C\left(|||u - \hat{u}_{\mathrm{CR}}|||_{D_T}^2 + |||u_{\mathrm{CR}} - \hat{u}_{\mathrm{CR}}|||_{D_T}^2 + \sum_{\hat{T}\subset\overline{D}_T} \frac{h_{\hat{T}}^2}{\alpha_{\hat{T}}}\|f - \Pi_1 f\|_{0;\hat{T}}^2\right).
\end{aligned}
$$

## 5. Comparison of the residual based error estimators

In this section, we will interpret the Crouzeix-Raviart finite element discretization as a mortar finite element method. We will denote the residual based error estimator obtained in the mortar context by $\eta_\mathrm{M}$ and the error estimator investigated for the Crouzeix-Raviart finite element discretization by $\eta_{\mathrm{CR}}$. The two estimators are compared, and the Lagrange multiplier $\lambda_\mathrm{M}$ and the normal derivative $a\nabla u_{\mathrm{CR}}\boldsymbol{n}_e$ are compared. For simplicity, we assume, for the rest of this section, that the exact Crouzeix-Raviart approximation $u_{\mathrm{CR}}$ is available and that the coefficients $a$ and $b$ are piecewise constant in the elements of the initial triangulation.

### *5.1. Crouzeix-Raviart finite elements – mortar finite elements*

The nonconforming Crouzeix-Raviart finite elements can be viewed as a mortar finite element discretization. In this case, each subdomain consists

of one triangle and the skeleton is the union of all edges

$$\overline{\Omega} = \bigcup_{T \in \mathcal{T}_l} T, \quad \mathcal{S} = \bigcup_{e \in \mathcal{E}_l} e.$$

The mortar finite element space is $X_h^{-1}(\Omega) \times W_h(\mathcal{S})$ where

$$X_h^{-1}(\Omega) := \prod_{T \in \mathcal{T}_l} P_1(T), \quad W_h(\mathcal{S}) := \prod_{e \in \mathcal{E}_l} P_0(e).$$

Thus, the elements of the Lagrange multiplier space are constants on each edge. The mortar finite element solution is given in terms of the following saddle point problem: Find $(u_{\rm M}, \lambda_{\rm M}) \in X_h^{-1}(\Omega) \times W_h(\mathcal{S})$ such that

$$\begin{aligned} a\,(u_{\rm M}, v) + b\,(\lambda_{\rm M}, v) &= (f, v)_0, \quad && v \in X_h^{-1}(\Omega), \\ b\,(\mu, u_{\rm M}) \qquad\quad &= 0, && \mu \in W_h(\mathcal{S}). \end{aligned} \tag{5.1}$$

Here, the bilinear forms $a\,(\cdot,\cdot)$ and $b\,(\cdot,\cdot)$ are given by

$$a\,(v, w) = \sum_{T \in \mathcal{T}_l} \int_T (a \nabla v \nabla w + bvw)\, dx, \quad b\,(\mu, v) = -\sum_{e \in \mathcal{E}_l} \int_e \mu\, [v]_J\, d\sigma.$$

In comparison to Sect. 2, we have modified the variational problem in one respect. The boundary of $\Omega$ is now part of the skeleton and thus, the homogeneous Dirichlet boundary condition is satisfied only in the weak form

$$\int_e u_{\rm M}\, d\sigma = 0, \quad e \in \partial\Omega.$$

The Lagrange multiplier can be eliminated locally, and we obtain the following positive definite variational problem: Find $u_{\rm M} \in X_h(\Omega)$ such that

$$a\,(u_{\rm M}, v) = (f, v)_0, \quad v \in X_h(\Omega) \tag{5.2}$$

where

$$X_h(\Omega) := \Big\{ v \in X_h^{-1}(\Omega) \,|\, \int_e [v]_J\, d\sigma = 0,\ e \in \mathcal{E}_l \Big\}.$$

Since $[v]_J$ is a linear function on $e$, the matching condition simply means that $v|_{T_i}(m_e) = v|_{T_{\rm o}}(m_e)$, $e = \partial T_i \cap \partial T_{\rm o}$ and $v|_{T_e}(m_e) = 0$, $e \subset \partial\Omega \cap \partial T_e$. Thus, the continuity of a piecewise linear ansatz function $v \in X_h(\Omega)$ at the midpoint of the edges is guaranteed,

$$X_h(\Omega) = CR(\Omega; \mathcal{T}_l),$$

and the variational problem (5.2) is exactly the same as (4.1) and therefore $u_{\mathrm{M}} = u_{\mathrm{CR}}$.

In the next step, we consider the first equation of the saddle point problem (5.1) in more detail. Let $\psi_{e;T} \in X_h^{-1}(\Omega)$, $e \subset \partial T$, be the nodal nonconforming basis function $\psi_e$ restricted to the element $T$. It is easy to see that

$$\lambda_{\mathrm{M}}|_e = \frac{-(\boldsymbol{n}_e, \boldsymbol{n}_T)}{h_e}(f - Lu_{\mathrm{CR}}, \psi_{e;T})_{0;T} + a\nabla u_{\mathrm{CR}}\boldsymbol{n}_e|_T, \quad T \subset \overline{D}_e. \tag{5.3}$$

Recall that the scalar product $(\boldsymbol{n}_e, \boldsymbol{n}_T)$ is equal to one if $T = T_i$ and to minus one, if $T = T_{\mathrm{o}}$. Thus, the Lagrange multiplier can be obtained easily by a local postprocessing of $u_{\mathrm{CR}}$. In particular, it can be expressed in terms of $u_{\mathrm{CR}}|_{T_i}$ or $u_{\mathrm{CR}}|_{T_{\mathrm{o}}}$.

### *5.2. A simplified residual based error estimator*

In this subsection, we will show that the two error estimators $\eta_{\mathrm{M}}$ and $\eta_{\mathrm{CR}}$ are locally equivalent. Taking (5.3) into account, we will introduce a simplified error estimator which only depends on the jump of $u_{\mathrm{CR}}$ and on $(f - Lu_{\mathrm{CR}})|_T$ but not on the jump of $a\nabla u_{\mathrm{CR}}\boldsymbol{n}_e$.

We recall that the estimator $\eta_{\mathrm{M}}$ is defined by (see Sect. 3):

$$\eta_{\mathrm{M};T}^2 = \frac{h_T^2}{\alpha_T}\|\Pi_1 f - Lu_{\mathrm{CR}}\|_{0;T}^2 + \sum_{j=1}^{3}\Big(\frac{h_{e_j}}{\alpha_T}\|a\nabla u_{\mathrm{CR}}|_T\boldsymbol{n}_{e_j} - \lambda_{\mathrm{M}}\|_{0;e_j}^2 + w_j\frac{\alpha_T}{h_{e_j}}\|[u_{\mathrm{CR}}]_J\|_{0;e_j}^2\Big),$$

where $e_j$, $1 \le j \le 3$, denote the edges of the element $T$, and $w_j$ is given by $w_j = \frac{1}{2}$, if $e_j$ is an inner edge and by $w_j = 1$, if $e_j$ is an edge on the boundary. Since each edge $e \in \mathcal{E}_l$ belongs to the skeleton, we do not have any interior edge in the sense of the definition of Sect. 3.

In contrast to Sect. 3, we will add the term $h_{e_j}^{-1}\|[u_{\mathrm{CR}}]_J\|_{0;e_j}^2$ to both subdomains $T_i$ and $T_{\mathrm{o}}$. If we change the orientation of $\boldsymbol{n}_e$, the sign of $\lambda_{\mathrm{M}}|_e$ will change, but we still obtain the same $u_{\mathrm{CR}}$. Therefore, we do not distinguish between $T_i$ and $T_{\mathrm{o}}$ in the definition of the error estimator.

In Sect. 4, the error estimator $\eta_{\mathrm{CR}}$ is defined by

$$\eta_{\mathrm{CR};T}^2 = \frac{h_T^2}{\alpha_T}\|\Pi_1 f - Lu_{\mathrm{CR}}\|_{0;T}^2 + \sum_{j=1}^{3}\Big(\hat{w}_j\frac{h_{e_j}}{\alpha_T}\|[a\nabla u_{\mathrm{CR}}\boldsymbol{n}_e]_J\|_{0;e_j}^2 + w_j\frac{\alpha_T}{h_{e_j}}\|[u_{\mathrm{CR}}]_J\|_{0;e_j}^2\Big),$$

where the weight $\hat{w}_j$ is given by $\hat{w}_j = \frac{2\alpha_{T_\mathrm{o}}\alpha_{T_i}}{(\alpha_{T_\mathrm{o}}+\alpha_{T_i})^2}$, if $e_j$ is an inner edge, $e_j = \partial T_i \cap \partial T_\mathrm{o}$ and by $\hat{w}_j = 1$, if $e_j$ is an edge on the boundary.

To obtain local equivalence between $\eta_{\mathrm{M};T}$ and $\eta_{\mathrm{CR};T}$, we have to consider $\|[a\nabla u_{\mathrm{CR}}\boldsymbol{n}_e]_J\|^2_{0;e}$ and $\|a\nabla u_{\mathrm{CR}}|_T\boldsymbol{n}_e - \lambda_{\mathrm{M}}\|^2_{0;e}$ in more detail. Equation (5.3) yields

$$a\nabla u_{\mathrm{CR}}|_T\boldsymbol{n}_e - \lambda_{\mathrm{M}}|_e = \frac{(\boldsymbol{n}_e,\boldsymbol{n}_T)}{h_e}(f - L\hat{u}_{\mathrm{CR}},\psi_{e;T})_{0;T},\ T \subset \overline{D}_e, \tag{5.4}$$

and thus $h_e\|a\nabla u_{\mathrm{CR}}|_T\boldsymbol{n}_e - \lambda_{\mathrm{M}}\|^2_{0;e} \le \frac{1}{6}h_T^2\|\Pi_1 f - L\hat{u}_{\mathrm{CR}}\|^2_{0;T}$. In addition,

$$\frac{h_e}{2}\|[a\nabla u_{\mathrm{CR}}\boldsymbol{n}_e]_J\|^2_{0;e} \le h_e\|a\nabla u_{\mathrm{CR}}|_{T_i}\boldsymbol{n}_e - \lambda_{\mathrm{M}}\|^2_{0;e} + \frac{1}{6}h_T^2\|\Pi_1 f - L\hat{u}_{\mathrm{CR}}\|^2_{0;T_\mathrm{o}}$$

holds for each $e \in \mathcal{E}_l \setminus \mathcal{E}_l^{\mathrm{B}}$. By definition $[a\nabla u_{\mathrm{CR}}\boldsymbol{n}_e]_J = 0$ for $e \in \mathcal{E}_l^{\mathrm{B}}$. Combining these formulas, we obtain the following estimate

$$\frac{2}{3}\eta^2_{\mathrm{M};T} \le \eta^2_{CR;T} \le \frac{3}{2}\eta^2_{\mathrm{M};T} + \sum_{i=1}^{i_T}\eta^2_{\mathrm{M};T_i},$$

where $T_i$, $1 \le i \le i_T \le 3$ are the neighbor elements of $T$.

Using (5.4), it is easy to see that the term $\|[a\nabla u_{\mathrm{CR}}\boldsymbol{n}_e]_J\|^2_{0;e}$, in the definition of the error estimator, is redundant and can be left out. The simplified error estimator $\hat{\eta}^2_{CR} := \sum_{T\in\mathcal{T}_l}\hat{\eta}^2_{CR;T}$ is then defined by

$$\hat{\eta}^2_{CR;T} := \frac{h_T^2}{\alpha_T}\|\Pi_1 f - Lu_{\mathrm{M}}\|^2_{0;T} + \sum_{j=1}^{3} w_j\frac{\alpha_T}{h_{e_j}}\|[u_{\mathrm{CR}}]_J\|^2_{0;e_j}.$$

**Theorem 5.1** *There exist constants* $0 < \hat{c}_{\mathrm{R}} \le \hat{C}_{\mathrm{R}}$ *and* $\hat{\gamma}_{\mathrm{R}} > 0$, *independent of the refinement level* $l \ge 1$ *such that*

$$\begin{aligned}
|\!|\!| u - u_{\mathrm{CR}} |\!|\!| &\le C_{\mathrm{R}}\left(\hat{\eta}_{\mathrm{CR}} + |\!|\!| f - \Pi_1 f |\!|\!|_{\mathcal{T}_l}\right),\\
|\!|\!| u - u_{\mathrm{CR}} |\!|\!| &\ge c_{\mathrm{R}}\left(\hat{\eta}_{\mathrm{CR}} - \hat{\gamma}_{\mathrm{R}}|\!|\!| f - \Pi_1 f |\!|\!|_{\mathcal{T}_l}\right).
\end{aligned}$$

*Proof.* These assertions are proved by using the definition of the error estimator, Theorem 4.3, and (5.4). □

## 6. Numerical results

In this section, we will present some numerical results illustrating the adaptive refinement process and the efficiency of the different error estimators. We consider the error estimator of Sect. 3 for the mortar situation as well as the error estimator introduced in Sect. 4 for the Crouzeix-Raviart discretization.

Starting from a coarse triangulation, the discretized problems are solved on each refinement level by a preconditioned iteration scheme, see [41] for the Crouzeix-Raviart case and [2,31] for the mortar method. The iteration process on level $l+1$ is stopped if the estimated iteration error $\epsilon_{l+1}$ satisfies $\epsilon_{l+1}^2 \leq 0.01\eta_l^2 \frac{N_l}{N_{l+1}}$ where $\eta_l$ is the estimated error on level $l$ and $N_l$ and $N_{l+1}$ stand for the number of nodes on level $l$ and $l+1$, respectively. In the mortar situation, we use the adaptive refinement process of Bänsch [10] which is based on a bisection strategy whereas, in the Crouzeix-Raviart setting, we use the refinement algorithm of Bank et. al. [11].

Both error estimators are applied to the following test example: $-\Delta u + 100u = f$ on $(0,1)^2$, where the right hand side $f$ and the Dirichlet boundary conditions are chosen so that the exact solution is $(2\cosh 10)^{-1}(\cosh(10x) + \cosh(10y))$. This solution has a pronounced boundary layer. We start with an initial triangulation consisting of four isosecles triangles.

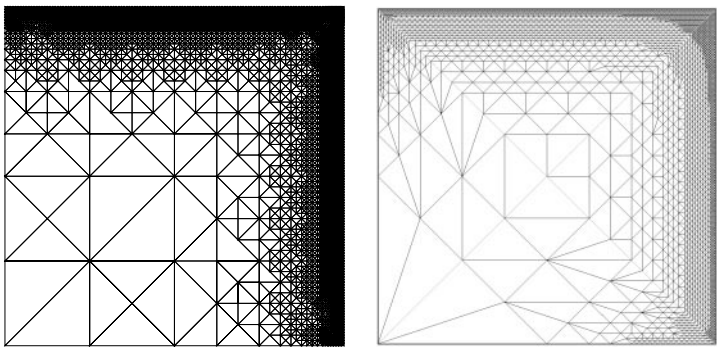

Mortar finite elements Crouzeix-Raviart finite elements

**Fig. 6.1.** Adaptive refined triangulations (Example 1)

In the mortar case, we also use this coarse triangulation to define the subdomains. Figure 6.1 shows the grids generated by adaption. Although the triangulations on the four subdomains are obtained independently, we get almost conforming triangulations at the interfaces $y = x$ and $y = 1 - x$. In such a situation, there is no real benefit from mortar finite element method.

The efficiency index is given in Fig. 6.2. It is asymptotically constant in both cases. For this problem, the error estimator for the Crouzeix-Raviart finite element discretization is more accurate than that of the mortar method.

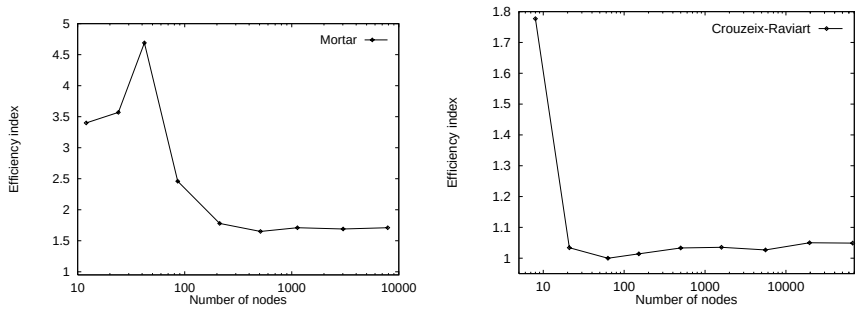


**Fig. 6.2.** Mortar (left) and Crouzeix-Raviart (right) finite elements (Example 1)

We next apply our error estimators to a second example with discontinuous coefficients. Here, we can see the advantage of the mortar discretization. We consider the elliptic equation $-\mathrm{div}\, a\nabla u = f$, on $(0,1)^2$, where the right hand side $f$ and the Dirichlet boundary conditions are chosen such that the exact solution is given by $(y-x)(1-x-y)(x-0.5)^2(y-0.5)^2/a$ and $a$ is discontinuous with $a = 1$ for $x < y < 1-x$ and $x > y > 1-x$ and $a = 100$ elsewhere.

For the mortar method, no matching of the triangulations is required across the skeleton. Strongly nonconforming global triangulations are generated by the adaptive refinement process (see left part of Fig. 6.3). In contrast, a conforming triangulation has to be produced in the Crouzeix-Raviart setting, and we observe a strong adaptive refinement on both sides of the

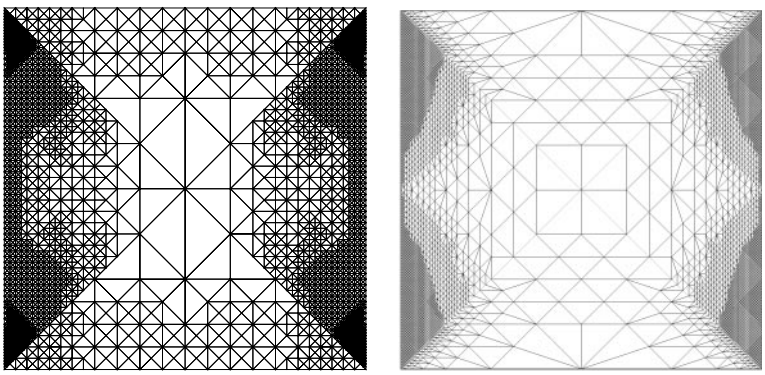

Mortar finite elements Crouzeix-Raviart finite elements

**Fig. 6.3.** Adaptive refined triangulations (Example 2)

**Table 6.1.** Estimated and true errors for the mortar finite element discretization (Example 2)

| level | nodes | estimated error | true error | eff. index |
|---|---|---|---|---|
| 0 | 24 | $0.259 \cdot 10^{-1}$ | $0.157 \cdot 10^{-1}$ | 1.65 |
| 1 | 42 | $0.911 \cdot 10^{-2}$ | $0.158 \cdot 10^{-1}$ | 0.578 |
| 2 | 60 | $0.869 \cdot 10^{-2}$ | $0.862 \cdot 10^{-2}$ | 1.01 |
| 3 | 126 | $0.456 \cdot 10^{-2}$ | $0.465 \cdot 10^{-2}$ | 0.979 |
| 4 | 206 | $0.265 \cdot 10^{-2}$ | $0.253 \cdot 10^{-2}$ | 1.05 |
| 5 | 454 | $0.153 \cdot 10^{-2}$ | $0.142 \cdot 10^{-2}$ | 1.08 |
| 6 | 1190 | $0.889 \cdot 10^{-3}$ | $0.828 \cdot 10^{-3}$ | 1.07 |
| 7 | 3470 | $0.511 \cdot 10^{-3}$ | $0.476 \cdot 10^{-3}$ | 1.07 |
| 8 | 9830 | $0.303 \cdot 10^{-3}$ | $0.281 \cdot 10^{-3}$ | 1.08 |

interfaces $y = x$ and $y = 1 - x$ (see right part of Fig. 6.3). On the sides where $a = 100$, this local refinement is caused by the refinement rules and not by the error estimator. In such a situation, mortar methods are better than standard finite element methods on conforming triangulations.

Table 6.1 gives the efficiency index as well as the error of the mortar finite element discretization. In contrast to the first example, the efficiency index tends to one with an increasing number of nodes.

## References


1. Abdoulaev, G., Kuznetsov, Y., Pironneau, O. (1996) The numerical implementation of the domain decomposition method with mortar finite elements for a 3D problem. Preprint, Laboratoire d'Analyse Numérique, Univ. Pierre et Marie Curie, Paris
2. Achdou, Y., Kuznetsov, Y. (1995) Substructuring preconditioners for finite element methods on nonmatching grids. East-West J. Numer. Math. **3**, pp. 1–28
3. Achdou, Y., Kuznetsov, Y., Pironneau, O. (1995) Substructuring preconditioners for the $Q_1$ mortar element method. Numer. Math. **71**, pp.419–449
4. Achdou, Y., Maday, Y., Widlund, O. (1996) Méthode iterative de sous-structuration pour les éléments avec joints. C. R. Acad. Sci., Paris, Ser. I **322**, pp. 185–190
5. Achdou, Y., Maday, Y., Widlund, O. (1997) Iterative Substructuring Preconditioners for Mortar Element Methods in Two Dimensions. Tech. Report 735, Courant Institute of Math. Sciences, New York
6. Alonso, A. (1996) Error estimators for a mixed method. Numer. Math. **74**, pp. 385–395
7. Arnold, D.N., Brezzi, F. (1985) Mixed and nonconforming finite element methods: implementation, post–processing and error estimates. $M^2AN$ Math. Modell. Numer. Anal. **19**, pp. 7–35
8. Babuška, I., Rheinboldt, W.C. (1978) Error estimates for adaptive finite element computations. SIAM J. Numer. Anal. **15**, pp. 736–754
9. Babuška, I., Rheinboldt, W.C. (1978) A posteriori error estimates for the finite element method. Int. J. Numer. Methods Eng. **12**, pp. 1597–1615
10. Bänsch, E. (1991) Local mesh refinement in 2 and 3 dimensions. IMPACT of Computing in Science and Engrg. **3**, pp. 181—191

11. Bank, R.E., Sherman, A.H., Weiser, A. (1983) Refinement algorithm and data structures for regular local mesh refinement. In: Scientific Computing, R. Stepleman et al. (eds.), p. 3-17, IMACS North–Holland, Amsterdam
12. Becker, R., Rannacher, R. (1995) Weighted a posteriori error control in FE methods. To appear in Proc. ENUMATH-95, Paris, Sept. 18-22
13. Becker, R., Rannacher, R. (1996) A feed-back approach to error control in finite element methods: Basic analysis and examples. East-West J. Numer. Math. **4**, pp. 237–264
14. Ben Belgacem, F. (1995) The Mortar finite element method with Lagrange multipliers. Preprint, Laboratoire d'Analyse Numérique, Univ. Pierre et Marie Curie, Paris
15. Ben Belgacem, F., Maday, Y. (1993) Non-conforming spectral method for second order elliptic problems in 3D. East-West J. Numer. Math. **1**, pp. 235–251
16. Bernardi, C., Maday, Y., Patera, A.T. (1993) Domain decomposition by the mortar element method. In: Asymptotic and numerical methods for partial differential equations with critical parameters. (H. Kaper et al., Eds.), pp. 269-286, Reidel, Dordrecht
17. Bernardi, C., Maday, Y., Patera, A.T. (1994) A new nonconforming approach to domain decomposition: The mortar element method. In: Nonlinear partial differential equations and their applications. (H. Brezis et al., Eds.), pp. 13-51, Paris
18. Bernardi, C., Maday, Y. (1995) Raffinement de maillage en elements finis par la methode des joints. C. R. Acad. Sci., Paris, Ser. I 320, No.3, pp. 373–377
19. Bornemann, F., Erdmann, B., Kornhuber, R. (1996) A posteriori error estimates for elliptic problems in two and three spaces dimensions. SIAM J. Numer. Anal, **33**, pp. 1188-1204
20. Braess, D., Klaas, O., Niekamp, R., Stein, E., Wobschal, F. (1995) Error indicators for mixed finite elements in 2-dimensional linear elasticity. Comput. Methods Appl. Mech. Eng., **127**, pp. 345-356
21. Braess, D., Verfürth, R. (1996) A posteriori error estimators for the Raviart-Thomas element. SIAM J. Numer. Anal. **33**, pp. 2431-2444
22. Carstensen, C., Jansche, S. A posteriori error estimates and adaptive mesh-refining for non-conforming finite element methods. Submitted to Numer. Math.
23. M.Casarin, Widlund, O. (1996) A hierarchical preconditioner for the mortar finite element method. ETNA **4**, pp. 75-88
24. Clément, Ph. (1975) Approximation by finite element functions using local regularization. RAIRO Anal. Numér. **2**, pp. 77-84
25. Dari, E., Duran, R., Padra, C., Vampa, V. (1996) A posteriori error estimators for nonconforming finite element methods. $M^2AN$ **30**, pp. 385-400
26. Estep, D., Eriksson, K., Hansbo, P., Johnson, C. (1995) Introduction to adaptive methods for differential equations. Acta Numerica **3**, pp. 105-158
27. Haase, G., Heise, B., Kuhn, M., Langer, U. (1995) Adaptive domain decomposition methods for finite and boundary element equations. Preprint 95-2, Institut of Mathematics, Johannes Kepler University, Linz
28. Hackbusch, W., Paul, R. (1997) Kopplung von Finite-Elemente- und Randelementmethoden für die numerische Simulation von piezokeramischen Strukturen. In: Mathematik - Schlüsseltechnologie für die Zukunft (K.-H. Hoffmann et al., Eds.), pp. 151-160, Springer-Verlag, Heidelberg
29. Hoppe, R.H.W., Wohlmuth, B. (1997) Adaptive multilevel techniques for mixed finite element discretizations of elliptic boundary value problems. SIAM J. Numer. Anal., **34**, pp. 1658-1687
30. Hoppe, R., Wohlmuth, B. A comparison of a posteriori error estimators for mixed finite element discretizations. To appear in Math. Comp.

31. Iliash, Y., Kuznetsov, Y., Vassilevski, Y. (1996) Efficient parallel solvers for two dimensional potential flow and convection-diffusion problems on nonmatching grids. Preprint 357, Institut of Mathematics, University Augsburg
32. Le Tallec, P., Sassi, T. (1995) Domain decomposition with nonmatching grids: Augmented Lagrangian approach. Math. Comput. **64**, pp. 1367-1396
33. Le Tallec, P., Sassi, T., Vidrascu, M. (1994) Three-dimensional domain decomposition methods with nonmatching grids and unstructured coarse solvers. In: Domain decomposition methods in scientific and engineering computing (D. Keyes et al., Eds.), pp. 61-74, Pennsylvania
34. Kuznetsov, Y., Wheeler, M.F. (1995) Optimal order substructuring preconditioners for mixed finite element methods on non-matching grids. East-West J. Numer. Math. **3**, pp. 127-143
35. Oswald, P. (1994) Multilevel Finite Element Approximations: Theory and Application. Teubner, Stuttgart
36. Pousin, J., Sassi, T. (1996) Adaptive finite element and domain decomposition with non matching grids. In: Proc. 2nd ECCOMAS Conf. on Numer. Meth. in Engrg., Paris, September 1996 (J.-A. Désidéri et al., Eds.), pp. 476-481, Wiley, Chichester
37. Scott, L.R., Zhang, Z. (1990) Finite element interpolation of nonsmooth functions satisfying boundary conditions. Math. Comp. **54**, pp. 483-493
38. Verfürth, R. (1989) A posteriori error estimators for the Stokes equations. Numer. Math. **55**, pp. 309-325
39. Verfürth, R. (1994) A posteriori error estimation and adaptive mesh-refinement techniques. J. Comp. Appl. Math. **50**, pp. 67-83
40. Verfürth, R. (1996) A review of a posteriori error estimation and adaptive mesh-refinement techniques. Teubner-Verlag, Stuttgart
41. Wohlmuth, B. (1995) Adaptive Multilevel–Finite–Elemente Methoden zur Lösung elliptischer Randwertprobleme. PhD thesis, TU München